Talanta 120 (2014) 255–261

Contents lists available at ScienceDirect

Talanta

journal homepage: www.elsevier.com/locate/talanta

Hierarchically imprinted mesoporous silica polymer: An efficient solid-phase extractant for bisphenol A

Wenjing Cheng, Haotian Ma, Li Zhang, Yan Wang *

Academy of Fundamental and Interdisciplinary Sciences, Harbin Institute of Technology, Harbin 150001, China

ARTICLE INFO

Article history:
Received 30 August 2013
Received in revised form
28 November 2013
Accepted 2 December 2013
Available online 17 December 2013

Keywords:
Molecular imprint
Mesoporous silica
Bisphenol A
Solid-phase extraction
Hierarchical structures

ABSTRACT

Improving the site accessibility of molecularly imprinted polymer (MIP) is one of the biggest challenges for application of MIP in solid-phase extraction (SPE). Hierarchically imprinted mesoporous silica polymer was prepared with semicovalently bond imprinting methods based on MCM-41 and SBA-15 mesostructures, aiming to improve the site accessibility of MIP and increase the efficiency of molecularly imprinted-SPE. Characterization and performance tests of the obtained products revealed that molecularly imprinted SBA-15 (MIP-SBA-15) not only retained the mesoporous structure of SBA-15, but also displayed excellent selectivity of MIP to the target molecule. As the MIP-SBA-15 were adopted as the adsorbents of solid-phase extraction for detecting bisphenol A in spiked water samples, the recoveries of spiked samples more than 87%, which reveals that the molecularly imprinted SBA-15 were efficient SPE adsorbents for bisphenol A.

1. Introduction

Molecular imprinting can be defined as the assembly of a cross-linked polymer matrix around an imprint molecule that is held in place, either covalently or noncovalently, by judiciously chosen functional monomers [1], and it is attracting widespread interest especially in solid-phase extraction (SPE) [2,3], chromatography [4], catalysis [5,6], chemical sensors [7–9], and drug delivery [10,11]. Molecularly imprinted polymer (MIP) can recognize the targeted molecule with high selectivity because it has excellent "memory" function to the template molecule. Molecular imprinting technique has shown attractive potential in SPE since it was used for drug determination by Sellergren [12].

Traditional molecularly imprinted solid-phase extraction (MISPE) sorbents are prepared by bulk polymerization or precipitation polymerization [13–17]. As we know, these kinds of MIPs exhibit high selectivity but low rebinding capacity, poor site accessibility to target species and leakage of template molecules, because the imprinted polymer matrices are usually thick and the template molecules are embedded in the matrices too deeply to be fully eluted. In order to overcome these drawbacks, the surface molecular imprinting (SMIP) and dummy template imprinting (DMIP) have been developed [18–24].

Surface molecular imprinting is localizing the recognition sites on the surface of MIP supporters such as silica microparticles [22,25,26]. SMIP greatly increases the efficiency of adsorption and desorption, reducing the leakage of the residual template to a great extent by reducing the diffusion length of template. However, this method does risk sacrificing the size and shape selectivity.

Dummy template imprinting is not obviously different with MIP, except that the template prepared for MIP is replaced by its structure analogue [18–20,23,27]. Therefore, DMIP does not solve the leakage of the residual template molecules radically, it is just avoid the interference of template molecules to target molecules. Moreover, the structure and size of cavity in DMIP does not match completely well with the target molecule, thus, the competitive selectivity of DMIP does decrease to some extent.

Therefore, the accessibility problem is one of the biggest challenges for application of MIP. If the accessibility problem is solved, the template molecules of MIP will be easily removed, and the problem for leakage of the residual template molecules will be eliminated. Introducing hierarchical structures to MIP is an efficient approach to solve those problems [28]. The mesoporous or macropores in MIP facilitate the diffusing of solvent and template, which makes the removal of template more easier, and which also makes the imprinting site combine with target molecule more readily. MCM-41 and SBA-15 are two common periodic mesoporous silicas, they have the same hexagonal close-packed channel pore structure but differ in surface area, pore diameter, and wall thickness. And, their high pore volume and nanosized pore wall thickness offer high accessibility for a target molecule.

In this study, based on MCM-41 and SBA-15 mesostructures, a semicovalently bond molecule for imprinting was incorporated into the skeletons of the mesoporous materials. This provides both

* Corresponding author. Tel.: +86 45 18 640 3719.
E-mail address: wangy_msn@hotmail.com (Y. Wang).

0039-9140/$ - see front matter © 2013 Elsevier B.V. All rights reserved.
http://dx.doi.org/10.1016/j.talanta.2013.12.001

better access to imprinted sites through wider channels and offer high surface area and short diffusion distances for better access to imprint sites than in bulk imprinting polymer. The chosen imprint molecule was bisphenol A (BPA), a well known endocrine disruptor that has received significant attention in recent years due to concern over its presence in a variety of environmental water and consumer products including food packaging, food storage containers, and baby bottle [8,29–38].

2. Materials and methods

2.1. Reagents and materials

Bisphenol A (BPA), tetracethylorthosilicate (TEOS), sodium hydroxide (NaOH) and cetyltrimethylammonium bromide (CTAB) were purchased from Sinopharm Chemical Reagent Co., Ltd. (3-Isocyanatopropyl)triethoxysilane (ICPTES) obtained from Huishi Biochemical Reagent (Shanghai China) Co., Ltd. Biphenol (BP) and acetic acid were purchased from Fuyu Fine Chemical (Tianjin China) Co., Ltd. Methanol, hydrochloric acid and ethanol absolute were obtained from Benchmark Chemical Reagent (Tianjin China). P123 was purchased from Aldrich.

2.2. Preparation of hierarchically imprinted mesoporous silica polymer

Fabrication procedure of hierarchically imprinted mesoporous silica polymer was consisted of two steps as showed in Fig. 1, and the detailed descriptions were as following.

2.2.1. Preparation of the precursor of BPA (BPAP)

BPAP was synthesized according to the reported procedure [1] Fig. 1a shows the scheme of BPAP preparation. BPA (2.751 g, 12 mmol) and ICPTES (5.97 mL, 24 mmol) were added to 30 mL of dry tetrahydrofuran (THF) in a round-bottomed flask and allowed to react with stirring under N_2 at 373 K for 24 h. The solvent was removed by rotary evaporator.

2.2.2. Preparation of imprinted mesoporous MCM-41(MIP-MCM-41)

NaOH solution was added to a CTAB solution at 313 K. A solution of BPAP and TEOS was added dropwise. The composition of the final aqueous solution was maintained in the range of BPAP/20TEOS/6CTAB/900NaOH/3000H_2O. After stirring for 2 h, the solution was placed in a Teflon-lined vessel and heated at 393 K for 48 h. CTAB was removed by Soxhlet extraction with ethanol for 20 h. In order to remove BPA, reaction product was suspended in dimethylsulfoxide (DMSO) in a round-bottomed flask. Several drops of distilled water were added, and the suspension was heated to 433 K for 8 h with stirring. The MIP-MCM-41 was isolated by filtration, rinsed with distilled water and ethanol, and then oven-dried (Fig. 1b).

Non-imprinted MCM-41 (NIP-MCM-41) was prepared identically but with ICPTES instead of BPAP. MCM-41 was prepared identically but without BPAP.

2.2.3. Preparation of imprinted mesoporous SBA-15 (MIP-SBA-15)

A stock template solution was prepared by mixing P123 and hydrochloric acid. A solution of BPAP and TEOS was added dropwisely. The composition of the final aqueous solution was maintained with the molar ratio of 2BPAP/40TEOS/P123/280HCl/10300H_2O. After stirring for 24 h, the solution was placed in a Teflon-lined vessel and heated at 353 K for 24 h. P123 was removed by Soxhlet extraction with ethanol for 20 h. BPA removed methods was the same as that of MIP-MCM-41.

Non-imprinted SBA-15 (NIP-SBA-15) was prepared identically but with ICPTES instead of BPAP. SBA-15 was prepared identically but without BPAP.

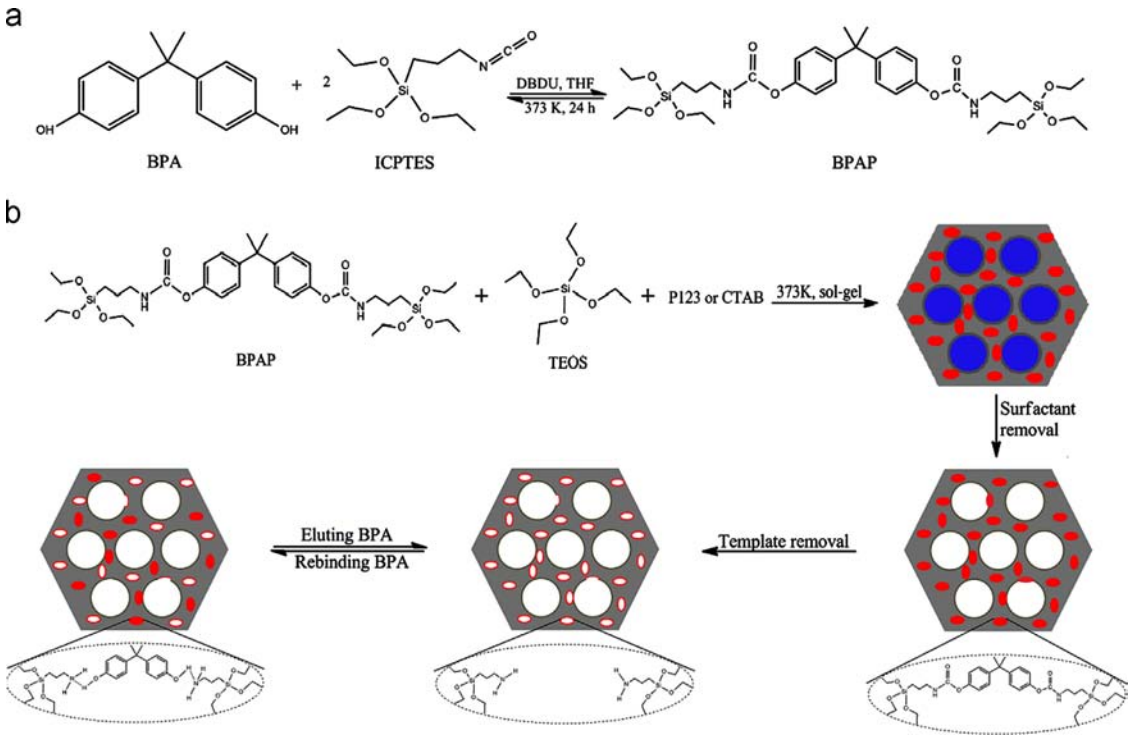

Fig. 1. Scheme for synthesis of BPAP (a) and imprinted mesoporous silica polymer (b).

2.3. Characterization and test of hierarchically imprinted mesoporous silica polymer

2.3.1. Characterization

Fourier transform infrared spectra (FTIR) were recorded on a Nicolet Avatar-360 instrument. Nitrogen adsorption was carried out on a Quantachrome Autosorb-1-c with a bath temperature of 77 K. Surface areas were determined using Brunauer–Emmett–Teller (BET) theory, and pore size distributions were calculated using Barrett–Joyner–Halenda (BJH) theory from the adsorption branch. Powder XRD patterns were measured on a STOE STADIP instrument with Cu$K\alpha$ radiation. HPLC (Agilent 1100) was used to determine BPA and BP. HPLC experimental condition was as follows: the mobile phase was consisted of water/methanol (30:70, v/v), the flow rate was maintained at 1.0 mL min^{-1}, the wavelength of ultraviolet detector was 282 nm. The concentrations of the BPA before and after the sorption were recorded by a TU-1800UV/Vis spectrophotometer.

2.3.2. Evaluation of sorption characteristic of hierarchically imprinted mesoporous silica polymer

The adsorption isotherms were obtained by suspending 30 mg hierarchically imprinted mesoporous silica polymer in 8 mL ethanol/water solution (2:3, v/v) with different BPA concentrations (0.1–1.0 mmol L^{-1}). Meanwhile, the adsorption kinetic curves were obtained by detecting the temporal evolution of BPA concentration (0.5 mmol L^{-1}) in the solutions.

The adsorption capacity Q(mg g^{-1}) is calculated according to the equation as follows:

$$Q = \frac{(c_o - c_f)v}{m}. \quad (1)$$

where C_o (mg mL^{-1}) and C_f (mg mL^{-1}) are the initial and final concentration of BPA, respectively, V (mL) is the total volume of the sample, and m (mg) is the mass of imprinted mesoporous materials.

The saturated adsorption capacity is obtained based on Langmuir adsorption equation as follows:

$$\frac{Ce}{Q} = \frac{Ce}{Q} + \frac{1}{KQ_{\max}} \quad (2)$$

where Q and Q_{max}(mg g^{-1}) are the experimental and theoretical saturated adsorption capacity of BPA, respectively, C_e(mg L^{-1}) is the corresponding concentration of BPA in solution, and K(L g^{-1}) is the Langmuir adsorption equilibrium constant.

The competitive adsorption was evaluated between BPA and its structure analogous (BP) with different concentration (0.2 and 0.4 mmol L^{-1}). The repeatability was tested by detecting the spiked sample five times using the same hierarchically imprinted mesoporous silica polymer.

2.3.3. Evaluation of hierarchically imprinted mesoporous silica polymer as SPE sorbents

Solid-phase extraction (SPE) is a useful separation technique that can be used to isolate desired compounds from an impure or mixed solution. MIP-SBA-15 was evaluated using a simplified SPE method. First 50 mg of MIP-SBA-15 was sandwiched between filter paper in a polyethylene syringe to create a simple SPE cartridge.

The extraction efficiency was affected by uploading rate and eluent, so different uploading rate and eluent were tested. BPA solution (0.1363 mmol L^{-1}) flow through the syringe with 0.1 mL min^{-1}, and collected every twenty minutes to estimate the breakthrough volume of MIP-SBA-15 and NIP-SBA-15. 4 mL of BPA solution with different concentration (0.1, 0.2, 0.3, 0.4 and 0.5 mmol L^{-1}) flow through the syringe with 0.1 mL min^{-1} to evaluate the capacity of SPE column.

3. Results and discussion

3.1. Characteristic of the FT-IR spectra

To verify that the expected products were obtained, their FTIR spectra were recorded and shown in Fig. 2. The carbamate C=O stretch at 1720 cm^{-1} is clearly visible for the BPAP, as-synthesized MIP(BPA)-MCM-41 and MIP(BPA)-SBA-15, revealing that BPAP was introduced into mesoporous materials. While it is weakened obviously for the as-synthesized MIP(BPA)-MCM-41 and MIP (BPA)-SBA-15, because the amount of BPAP is only ten percent of the total silicon source. No isocyanate (CNO) stretch appears at 2270 cm^{-1} in the MIP-MCM-41 spectrum, showing that the thermal bond cleavage does not regenerate the original NCO group and indicating that the carbamate is indeed converted to a primary amine. The NH_2 bending mode at about 1670 cm^{-1} overlaps with an OH bending mode at 1640 cm^{-1}, but it can still be identified by the unsymmetry of the peak.

3.2. Characteristic of the XRD spectra

Fig. 3 shows the small-angle X-ray diffraction (XRD) data obtained for each of the samples. Both pure mesoporous silica and their corresponding MIPs show typical peaks at small-angle range, which demonstrate the ordered mesoporous structures were formed. Comparing with pure MCM-41 and SBA-15, the intensity of peaks of MIP-MCM-41 and MIP-SBA-15 become weakened, indicating the long-range order of MIP-MCM-41 and MIP-SBA-15 were decreased because of the introduced BPAP. However, the hierarchically imprinted mesoporous silica polymer still maintains ordered mesostructure, and the abundant mesopores can improve diffusivity of molecular imprinting polymer.

3.3. Adsorption capacity of hierarchically imprinted mesoporous silica polymer

We compared the adsorption capacity of MIP-mesoporous silica polymer for BPA with NIP-mesoporous silica polymer and mesoporous silica polymer (Figs. 4 and 5). Fig. 4a shows the adsorption kinetic curves of BPA over samples MIP-SBA-15, MIP-MCM-41, NIP-SBA-15, NIP-MCM-41, SBA-15 and MCM-41. Compared with NIP-SBA-15 and SBA-15 (or NIP-MCM-41 and MCM-41), it is evidential that a much higher adsorption capacity was achieved on MIP-SBA-15 (or MIP-MCM-41), indicating that molecular imprinting sites integrate with long-range ordered

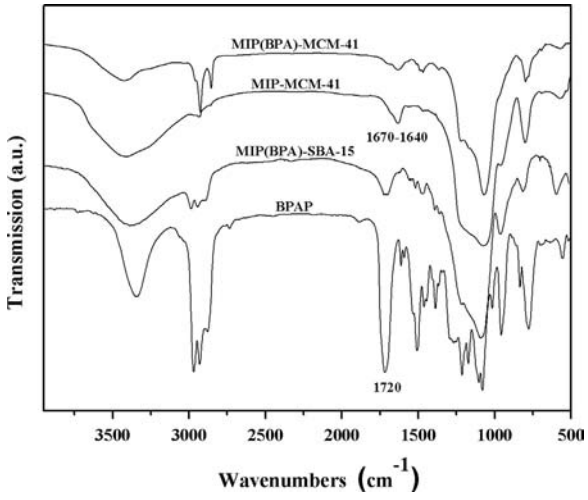

Fig. 2. FT-IR spectra of MIP(BPA)-MCM-41, MIP-MCM-41, MIP(BPA)-SBA-15 and BPAP.

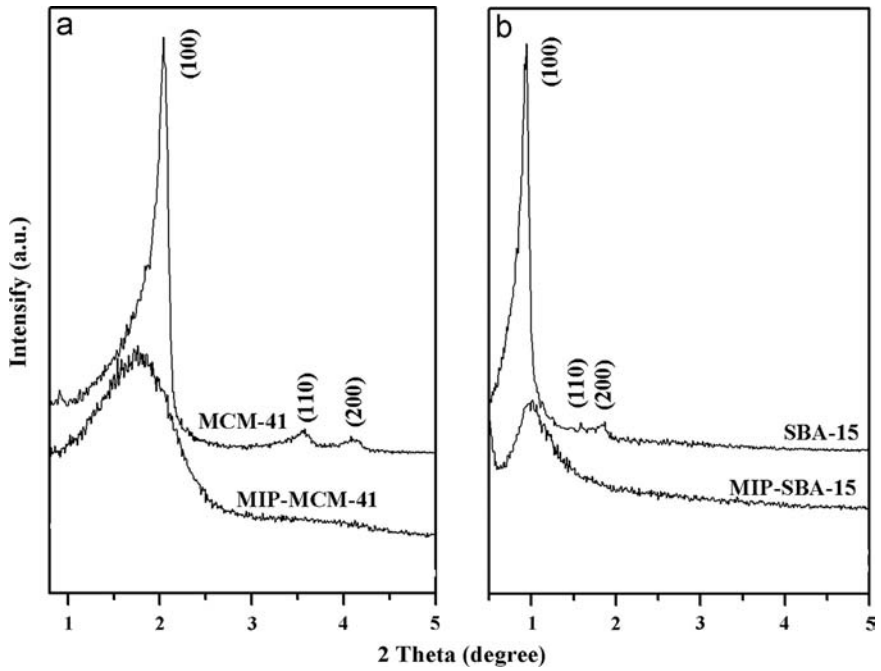

Fig. 3. X-ray diffraction plots for MCM-41 and MIP-MCM-41 (a), and SBA-15 and MIP-SBA-15 (b).

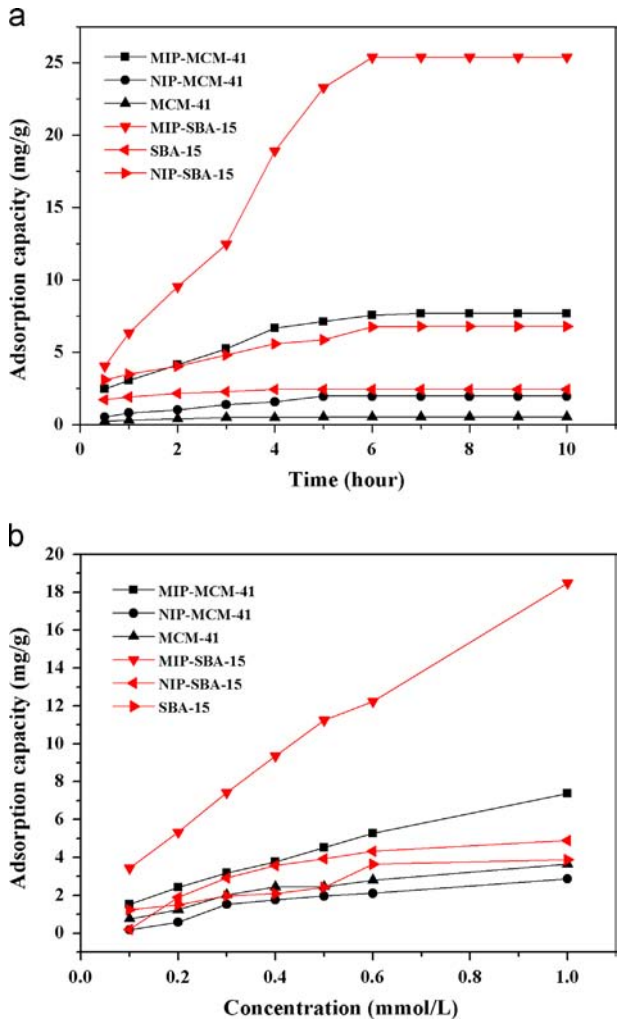

Fig. 4. Adsorption kinetic (a) and static adsorption curves (b) of BPA on MIP-MCM-41, NIP-MCM-41, MCM-41, MIP-SBA-15, NIP-SBA-15 and SBA-15.

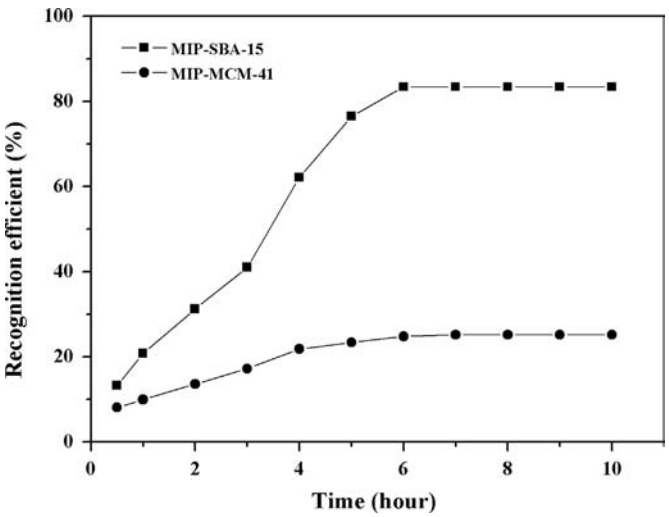

Fig. 5. Recognition efficient of MIP-SBA-15 and MIP-MCM-41.

mesoporous material successfully, and the molecular recognition capability of mesoporous material has been improved enormously. MIP-mesoporous material reached adsorption equilibrium at 6 h, while traditional molecular imprinted material had to take at least 48 h to arrive adsorption equilibrium, further demonstrating that MIP-mesoporous material overcome the defect of embedding imprint site in traditional MIP, and mesoporous facilitated target molecule binding with imprinted sites greatly.

The static adsorption of BPA on MIP-mesoporous silica were further compared (Fig. 4a). Based on Langmuir adsorption equation, the saturated adsorption capacity of MIP-SBA-15, MIP-MCM-41, NIP-SBA-15, NIP-MCM-41, SBA-15 and MCM-41 were 24.84, 13.70, 10.68, 5.85, 11.93 and 6.98 mg g^{-1}, respectively. The theoretical saturated adsorption of MIP-mesoporous silica was about 2.5 times as much as that of NIP-mesoporous silica, confirming that molecular imprinting sites integrate with mesoporous material again. The fact that the Q_{max} of NIP-mesoporous silica smaller

than mesoporous silica attributed to the ICPTES, which destroyed the long-range ordered structure of mesoporous silica somewhat.

Fig. 5 shows the recognition capability of MIP-SBA-15 is four-fold of MIP-MCM-41, suggesting that the structure of mesoporous matrix influence the recognition efficient greatly. Both SBA-15 and MCM-41 are mesoporous material, but the pore diameter of SBA-15 is bigger than MCM-41, which facilitated target molecular diffusing into meso-channels and bonding with imprinted sites.

3.4. Competitive selectivity of hierarchically imprinted mesoporous silica polymer

To evaluate the competitive selectivity of MIP-SBA-15, MIP-MCM-41, NIP-SBA-15 and NIP-MCM-41, solutions of BPA/BP (structure shown in Fig. 6a) with different concentration were prepared as the extracted samples. Fig. 6b shows that the competitive selectivity of imprinted mesoporous silica is superior to the non-imprinted, and the molecular recognition properties of MIP-SBA-15 is better than MIP-MCM-41, indicating that MIP-SBA-15 is an ideal extractant for separation of bisphenol A.

3.5. N_2 adsorption–desorption of MIP-SBA-15 and NIP-SBA-15

The porosity of MIP-SBA-15 and NIP-SBA-15 were investigated by a nitrogen adsorption–desorption experiment. Fig. 7a and b shows type IV curves indicating that the pore sizes of MIP-SBA-15 and NIP-SBA-15 are in the mesopores range. Table 1 shows that the Brunauer–Emmett–Teller (BET) surface area, Barret–Joyner–Halenda (BJH) pore size and pore volume of NIP-SBA-15 are bigger than that of MIP-SBA-15. Generally, the more bigger the BET surface area, BJH pore size and pore volume the more stronger of the adsorbability. However, the adsorbability of MIP-SBA-15 to BPA is better than NIP-SBA-15 due to the exist of molecularly imprinted sites. So the imprinted SBA-15 possess the binding specificity of MIP.

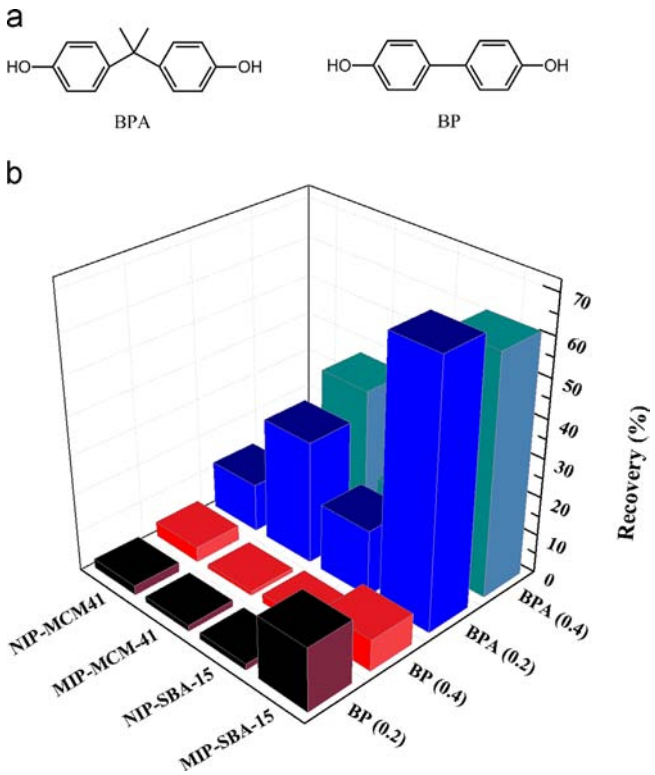

Fig. 6. Molecular structure of BPA and BP (a), and competitive selectivity of MIP-SBA-15, NIP-SBA-15, MIP-MCM-41 and NIP-MCM-41 to BPA ($n=3$).

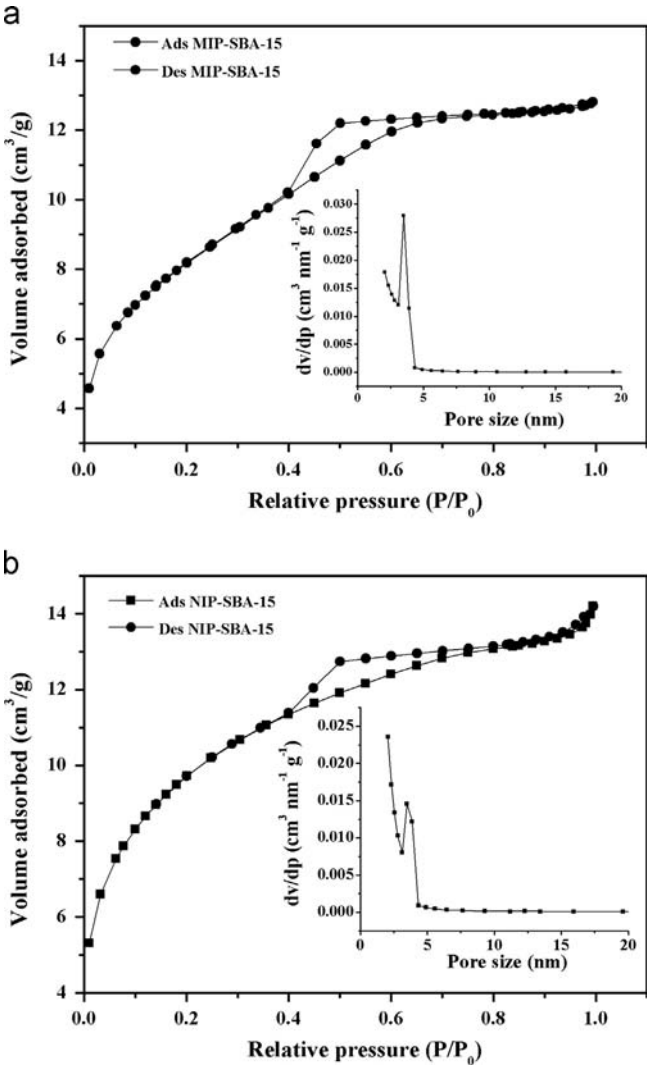

Fig. 7. N_2 adsorption and desorption isotherms of MIP-SBA-15 (a) and NIP-SBA-15 (b).

Table 1
Physicochemical properties of MIP-SBA-15 and NIP-SBA-15.

Materials	BET surface area ($m^2\ g^{-1}$)	BJH pore size (nm)	Pore volume ($cm^3\ g^{-1}$)	Pore wall thickness (nm)
MIP-SBA-15	640.3	3.0	0.4397	4.575
NIP-SBA-15	743.2	4.0	0.4731	3.971

3.6. Stability of MIP-SBA-15

To evaluate the stability of MIP-SBA-15, the same MIP-SBA-15 was reused five times for binding/removing BPA. Repeated binding/removing tests showed that the recovery decreased as cycle continued, but the recovery of the third time was still more than 80% (Fig. 8), which suggested that MIP-SBA-15 have good stability and reusability, even though some imprinted sites might have been broken during eluting of BPA.

3.7. Evaluation of MIP-SBA-15 as SPE sorbents

3.7.1. Effect of uploading rate

Sample flow rate affected the time of contact between target analyte and SPE sorbents. Theoretically, lower sample loading flow

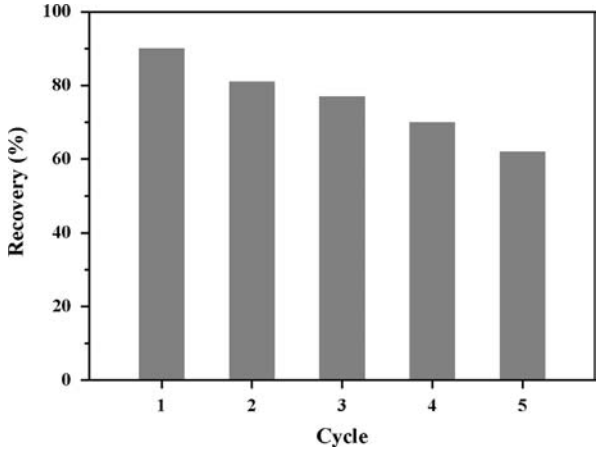

Fig. 8. Recoveries of BPA on recycling MIP-SBA-15 ($n=3$).

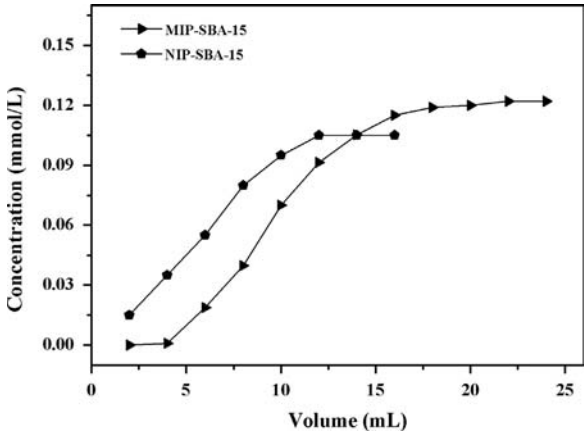

Fig. 9. Breakthrough volume of MIP-SBA-15 and NIP-SBA-15 SPE cartridge.

Table 2
Effect of sample loading flow rate on the recovery of BPA using MI-SPE.

Uploading rate (mL min^{-1})	Sample volume (mL)	Spiked level (mmol L^{-1})	Recovery (%)
0.10	4	0.1361	92.75
0.15	4	0.1361	89.13
0.20	4	0.1361	82.33
0.25	4	0.1361	75.97
0.30	4	0.1361	69.94

Table 3
Effect of different elution to recovery efficiency.

Eluent (v/v)	Eluent volume (mL)	Spiked level (mmol L^{-1})	Recovery (%)
Water/methanol (1/0)	3	0.1361	10.91
Water/methanol (5/1)	3	0.1361	75.49
Water/methanol (5/5)	3	0.1361	89.02
Methanol/acetic acid (9/1)	3	0.1361	96.54

rate could maximize their interaction, thus may enhance the preconcentration performance. A volume of 4.0 mL working standard solutions (0.1361 mmol L^{-1}) were preconcentrated in MIP-SBA-15 SPE at different flow rates (0.1, 0.15, 0.2, 0.25 and 3.0 mL min^{-1}). The results are shown in Table 2. The recoveries of BPA were declined as the uploading rate increased. Considering the purpose of improvement of extraction efficiency, the uploading rate of 0.1 mL min^{-1} was selected.

3.7.2. *Effect of eluent*

The appreciate elution condition should ensure analyte to be completely eluted from MI-SPE. The choice of eluents was one of the most crucial decisions to be made. MI-SPE loaded with BPA was washed with different eluent. The results are shown in Table 3. The recovery of BPA was increased with increasing the percent of methanol. However, the biggest recovery was obtained when using methanol/acetic acid (v/v 9/1) as eluent due to the replacement of acetic acid to BPA. Therefore, eluent was established as methanol/acetic acid (v/v 9/1).

3.7.3. *Breakthrough volume of MIP-SBA-15 SPE cartridge*

Breakthrough volume is an important factor which indicates the enrichment ability of a SPE column for the target analyte at a specific concentration. Fig. 9 shows the breakthrough volume of MIP-SBA-15 and NIP-SBA-15 SPE cartridge. The uploading concentration of BPA was 0.1361 mmol L^{-1}. The breakthrough volume of MIP-SBA-15 is 6 mL, which is about 3 times as much as that of NIP-SBA-15 (2 mL) due to the exist of BPA-imprinted sites. Therefore, the breakthrough volume of MIP-SBA-15 further proved that MIP-SBA-15 is an efficient solid phase extractant for BPA.

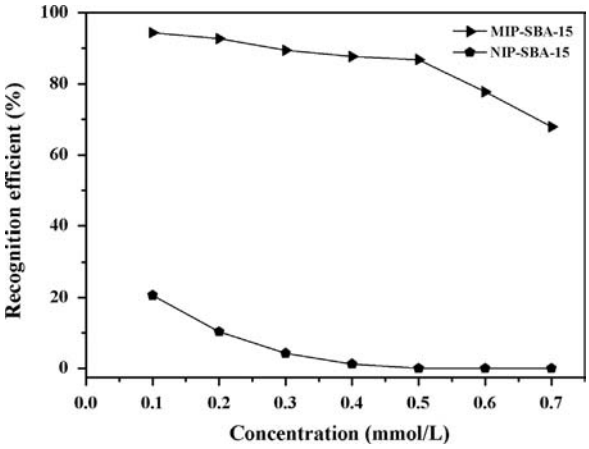

Fig. 10. Capacity of MIP-SBA-15 and NIP-SBA-15 SPE cartridge.

3.7.4. *Capacity of MIP-SBA-15 SPE cartridge*

Fig. 10 shows the capacity of MIP-SBA-15 and NIP-SBA-15 SPE cartridge. The recognition efficient of MI-SPE for BPA is still 86.84% when the concentration of BPA is 0.5 mmol L^{-1}. The maximum of MI-SPE is 4.43 mmol g^{-1}. However, the recognition efficient of MI-SPE to BPA less than 20% even the concentration of BPA is only 0.1 mmol L^{-1}. Which indicate that MIP-SBA-15 SPE cartridge is an efficient SPE for BPA.

3.8. *MIP-SBA-15 SPE cartridge for spiked water samples*

Water samples was selected for spiked analysis for validation of the method. The spiked concentrations for BPA at five levels (Table 4). They were subjected to extraction by the MIP-SBA-15 SPE cartridge, and then analyzed by HPLC. As shown in Table 4, the recoveries of BPA in these spiked samples ranged from 87.70 to 94.43%, suggesting that MIP-SBA-15 can be used as efficient SPE adsorbents for BPA extraction from aqueous solutions

Table 4
Determination of BPA in spiked water samples ($n=3$).

Samples	Spiked level (mmol L^{-1})	Recovery (%)
Water	0.1	94.43
Water	0.2	92.74
Water	0.3	89.45
Water	0.4	87.70

4. Conclusion

In this study, BPA imprinted mesoporous silica has been developed to synthesize hierarchical materials. As expected, the MIP-SBA-15 not only showed high selectivity to target molecule because of the existence of molecularly imprinted sites, but also displayed fast kinetic binding for the target molecule due to its porous structure and the thin wall thickness. Imprinting in the thin wall of SBA-15 improve the site accessibility to target species compared with bulk MIP by shorter the diffusion distances for BPA to imprinted sites. These MIP-SBA-15 were also applied for detecting BPA in spiked water samples, and the experimental results revealed that MIP-SBA-15 were efficient SPE adsorbents for BPA.

Acknowledgements

The authors thank the support from National Natural Science Foundation of China (No. 21273057 and No. 21075025) and support from Natural Science Foundation of Heilongjiang Province (No. B200910).

References

[1] J.E. Lofgreen, I.L. Moudrakovski, G.A. Ozin, Acs Nano 5 (2011) 2277.
[2] W.H. Zhao, N. Sheng, R. Zhu, F.D. Wei, Z. Cal, M.J. Zhai, S.H. Du, Q. Hu, J. Hazard. Mater. 179 (2010) 223.
[3] H.Y. Yan, F. Wang, H. Wang, G.L. Yang, J. Chromatogr. A 1256 (2012) 1.
[4] R.J. Ansell, J.K.L. Kuah, D.W. Wang, C.E. Jackson, K.D. Bartle, A.A. Clifford, J. Chromatogr. A 1264 (2012) 117.
[5] V. Abbate, A.R. Bassindale, K.F. Brandstadt, P.G. Taylor, J. Catal. 284 (2011) 68.
[6] A. Visnjevski, R. Schomacker, E. Yilmaz, O. Bruggemann, Catal. Commun. 7 (2006) 114.
[7] D.C. Apodaca, R.B. Pernites, R. Ponnapati, F.R. Del Mundo, R.C. Advincula, Macromolecules 44 (2011) 6669.
[8] M.C. Cela-Perez, M.M. Castro-Lopez, A. Lasagabaster-Latorre, J.M. Lopez-Vilarino, M.V. Gonzalez-Rodriguez, L.F. Barral-Losada, Anal. Chim. Acta 706 (2011) 275.
[9] N. Wu, L.A. Feng, Y.Y. Tan, J.M. Hu, Anal. Chim. Acta 653 (2009) 103.
[10] C. Alvarez-Lorenzo, F. Yanez, A. Concheiro, J. Drug Delivery Sci. Technol. 20 (2010) 237.
[11] R. Del Sole, M.R. Lazzoi, G. Vasapollo, Drug Delivery 17 (2010) 130.
[12] B. Sellergren, Anal. Chem. 66 (1994) 1578.
[13] D.K. Alexiadou, N.C. Maragou, N.S. Thomaidis, G.A. Theodoridis, M.A. Koupparis, J. Sep. Sci. 31 (2008) 2272.
[14] V. Pichon, F. Chapuis-Hugon, Anal. Chim. Acta 622 (2008) 48.
[15] H. Sambe, K. Hoshina, J. Haginaka, J. Chromatogr. A 1152 (2007) 130.
[16] K.G. Yang, B.Q. Li, H. Zhou, J.J. Ma, P.L. Bai, C.S. Zhao, J. Appl. Polym. Sci. 106 (2007) 2791.
[17] B.Y. Zu, G.Q. Pan, X.Z. Guo, Y. Zhang, H.Q. Zhang, J. Polym., Sci. Pol. Chem 47 (2009) 3257.
[18] H.Y. Yan, G.L. Cheng, G.L. Yang, J. Agric. Food Chem. 60 (2012) 5524.
[19] L. Zhang, F. Han, Y.Y. Hu, P. Zheng, X. Sheng, H. Sun, W. Song, Y.N. Lv, Anal. Chim. Acta 729 (2012) 36.
[20] Y.M. Yin, Y.P. Chen, X.F. Wang, Y. Liu, H.L. Liu, M.X. Xie, J. Chromatogr. A 1220 (2012) 7.
[21] W.H. Zhao, N. Sheng, R. Zhu, F.D. Wei, Z. Cal, M.J. Zhai, S.H. Du, Q. Hu, J. Hazard. Mater. 179 (2010) 223.
[22] X.Z. Xu, S.X. Chen, Q.H. Wu, J. Colloid Interface Sci. 385 (2012) 193.
[23] Z.K. Lin, W.J. Cheng, Y.Y. Li, Z.R. Liu, X.P. Chen, C.J. Huang, Anal. Chim. Acta 720 (2012) 71.
[24] X.G. Hu, J.L. Pan, Y.L. Hu, G.K. Li, J. Appl. Polym. Sci. 120 (2011) 1266.
[25] D. Dechtrirat, K.J. Jetzschmann, W.F.M. Stocklein, F.W. Scheller, N. Gajovic-Eichelmann, Adv. Funct. Mater. 22 (2012) 5231.
[26] W.Z. Xu, W. Zhou, W.H. Huang, J.M. Pan, H. Li, X.Y. Wu, Y.S. Yan, Microchim. Acta 175 (2011) 167.
[27] Z.G. Xu, Z.M. Liu, B.M. Yang, F.T. Zi, Prog. Chem. 24 (2012) 1592.
[28] A. Katz, M.E. Davis, Nature 403 (2000) 286.
[29] B. Shao, H. Han, X.M. Tu, L. Huang, J. Chromatogr. B 850 (2007) 412.
[30] K. Schoringhumer, M. Cichna-Markl, J. Chromatogr. B 850 (2007) 361.
[31] M.A. Rahman, M.J.A. Shiddiky, J.S. Park, Y.B. Shim, Biosens. Bioelectron. 22 (2007) 2464.
[32] K. Poouthree, W. Soonthorntantikul, N. Leepipatpiboon, A. Petsom, T. Nhujak, Electrophoresis 28 (2007) 3705.
[33] A. Ballesteros-Gomez, F.J. Ruiz, S. Rubio, D. Perez-Bendito, Anal. Chim. Acta 603 (2007) 51.
[34] M.H. Piao, H.B. Noh, M.A. Rahman, M.S. Won, Y.B. Shim, Electroanalysis 20 (2008) 30.
[35] F. Canale, C. Cordero, C. Baggiani, P. Baravalle, C. Giovannoli, C. Bicchi, J. Sep. Sci. 33 (2010) 1644.
[36] E. Turiel, A. Martin-Esteban, Anal. Chim. Acta 668 (2010) 87.
[37] L. Wang, W.C. Schnute, LC GC Eur. (2010) 7.
[38] A. Maroto, P. Kissingou, A. Diascorn, B. Benmansour, L. Deschamps, L. Stephan, J.Y. Cabon, P. Giamarchi, Anal. Bioanal. Chem. 401 (2011) 3011.